

the degree of crystallinity should be highly cognizant of the possible effects of sample preparation in their systems.

Acknowledgment. We thank the National Science Foundation for support of this work through Grant CPE-8008060. The critical comments and suggestions offered by Drs. Ian R. Harrison and Michael M. Coleman are also gratefully acknowledged.

References and Notes

- (1) Olabisi, O.; Robeson, L. M.; Shaw, M. T. "Polymer-Polymer Miscibility"; Academic Press: New York, 1979.
- (2) Nishi, T.; Wang, T. T. *Macromolecules* 1975, 8, 909.
- (3) Runt, J. P. *Macromolecules* 1981, 14, 420.
- (4) Kwei, T. K.; Frisch, H. L. *Macromolecules* 1978, 11, 1268.
- (5) Walsh, D. J.; McKeown, J. G. *Polymer* 1980, 21, 1330.
- (6) Shultz, R.; Young, A. L. *Macromolecules* 1980, 13, 663.
- (7) Berghmans, H.; Overbergh, N. *J. Polym. Sci., Polym. Phys. Ed.* 1977, 15, 1757.
- (8) Robeson, M. *J. Appl. Polym. Sci.* 1973, 17, 3607.
- (9) Seefried, C. G., Jr.; Koleske, J. V. *J. Test. Eval.* 1976, 4, 220.
- (10) Crescenzi, V.; Manzini, G.; Calzolari, G.; Borri, C. *Eur. Polym. J.* 1972, 8, 449.
- (11) Flick, J. R.; Petrie, S. E. B. In *Stud. Phys. Theor. Chem.* 1978, 10, 145.
- (12) (a) Richardson, M. J.; Savill, N. G. *Polymer* 1977, 18, 413. (b) *Ibid.* 1975, 16, 753.
- (13) Harrison, I. R.; Runt, J. *J. Polym. Sci., Polym. Phys. Ed.* 1979, 17, 321.
- (14) Runt, J.; Harrison, I. R. *Methods Exp. Phys.* 1980, 16B, Chapter 9.
- (15) Rebenfeld, L.; Makarewicz, P. J.; Weighman, H.-D.; Wilkes, G. L. *J. Macromol. Sci., Rev. Macromol. Chem.* 1976, C15, 279.
- (16) Rim, P. B.; Runt, J. P., to be submitted for publication.
- (17) Ong, C. J.; Price, F. P. *J. Polym. Sci., Polym. Symp.* 1978, No. 63, 45.

Restricted Flexing of Once-Broken Rods

Karl Zero and R. Pecora*

Department of Chemistry, Stanford University, Stanford, California 94305.
Received November 30, 1981

ABSTRACT: A theory for the dynamic light scattering intensity time correlation functions of dilute solutions of once-broken rods is developed. The rods are assumed to be small enough so that intramolecular interference can be neglected and the amount of bending at the joint is restricted to some maximum angle. Both polarized and depolarized correlation functions are calculated. The theory is then applied to the myosin rod, yielding a maximum angle of 128° (within the range 121 – 132°), a bending constant (D_r) of 24 ± 6 krad/s, and an overall rotational diffusion coefficient of 4.8 ± 0.8 krad/s. The values obtained are in good agreement with the known structure and size of the rod.

Introduction

Numerous authors have dealt with the motions of a once-broken rod and the effect of these motions on the dynamic light scattering correlation functions, primarily on a theoretical basis.¹⁻⁸ However, those papers assumed that the break point was a universal joint, allowing all possible angles between the two segments. Furthermore, the dynamic light scattering theories deal only with the isotropic scattering and intramolecular scattered light interference effects. In this work, an approximate theory is presented for the scattered light intensity time correlation functions from a dilute solution of once-broken rods. Both the isotropic and anisotropic components are found, assuming negligible intramolecular interference, and the angle between segments is restricted to some maximum value.

An example of a once-broken rod with a restricted intersegmental angle may be the myosin rod. The myosin molecule (Figure 1) is composed of three basic functional units.⁹⁻¹² The light meromyosin fragment (LMM) is believed to be rather stiff and rodlike. Subfragment 2 (S-2) is more flexible and connects the LMM with the head group. The head group consists of two subfragment 1 (S-1) moieties. The myosin rod is the myosin molecule with the head group removed. Both electric birefringence⁹ and electron microscopy^{11,12} experiments on the myosin rod and the myosin molecule indicate a considerable amount of flexibility at the joint between the LMM and S-2 fragments, with a possible maximum intersegmental angle of 145° (ref 12, where an angle of 0° means a stiff rod with no bend). Here, the results from dynamic light scattering experiments¹³ are compared with our theory of the once-broken rod in an attempt to extract the translational and

rotational diffusion coefficients and the maximum intersegmental angle.

Theory of the Dynamic Light Scattering Correlation Functions for a Once-Broken Rod

In the model used here, the motion between the two segments of a once-broken rod is restricted so that the largest angle the rod can bend at the joint is θ^0 (see Figure 2). For small θ^0 , a good approximation would be to assume that the bending motion is uncorrelated with the overall translation and rotation. In other words, the broken rod has about the same rotational and translational diffusion coefficients as the unbroken rod but with an additional time dependence of the total polarizability due to the bending motion. For large θ^0 , one would expect coupling between all three motions; however, if the bending motion is fast relative to the overall motions (which would be expected for long, thin rods), the assumption of uncorrelated motions should at least yield results that are semi-quantitatively correct. Higher order corrections to these approximations would probably be small relative to the experimental errors in the dynamic light scattering results (see Appendix).

The spectral density of the scattered light is determined by the autocorrelation function of the polarizability fluctuations. For dilute solutions of identical molecules, for which only self-correlations need to be considered, the polarizability time autocorrelation function is given by the equation¹⁴

$$I_{if}^a(q, t) = \langle N \rangle \langle \alpha_{if}^*(0) \alpha_{if}(t) \exp(i\vec{q} \cdot (\vec{r}(t) - \vec{r}(0))) \rangle \quad (1)$$

The brackets indicate ensemble averages. N is the number of molecules in the scattering volume, \vec{q} is the scattering

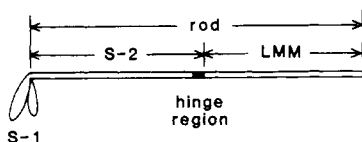


Figure 1. Scale diagram of the myosin molecule. Two S-1 moieties are attached to the rod portion, which consists of the LMM and S-2 fragments connected by a flexible hinge.

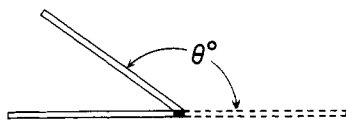


Figure 2. Bending motion of the myosin rod. θ^0 is the maximum bending angle.

vector (with length $q = (4\pi n/\lambda) \sin(\theta_s/2)$, where λ is the wavelength of the light, n is the refractive index of the scattering medium, and θ_s is the scattering angle), and $\vec{r}(t) - \vec{r}(0)$ is the displacement of a molecule in time t . The quantity α_{if} is the projection of the molecular polarizability tensor $\tilde{\alpha}$ onto the initial (\hat{n}_i) and final (\hat{n}_f) polarization directions of the light wave ($\alpha_{if} = \hat{n}_i \cdot \tilde{\alpha} \cdot \hat{n}_f$). If we assume statistical independence of the center of mass position and the orientation of the molecule, eq 1 can be simplified to the expression

$$I_{if}^\alpha(q, t) = \langle N \rangle \langle \alpha_{if}^*(0) \alpha_{if}(t) \rangle F_s(q, t) \quad (2)$$

where $F_s(q, t) = \langle \exp(i\vec{q} \cdot (\vec{r}(t) - \vec{r}(0))) \rangle$ is the self intermediate scattering function. For rods with length L short compared to q^{-1} ($qL < 4$), $F_s(q, t) = \exp(-q^2 D t)$, where D is the translational diffusion coefficient. If we choose our laboratory axes such that the incident light is somewhere in the x - y plane and the scattered light is along the x axis, the expressions for the polarized ($I_{VV}^\alpha(q, t)$, $\hat{n}_i = \hat{n}_f = \hat{z}$) and depolarized ($I_{VH}^\alpha(q, t)$, $\hat{n}_i = \hat{z}$, $\hat{n}_f = \hat{y}$) scattered light are

$$I_{VV}^\alpha = \langle N \rangle \langle \alpha_{zz}^*(0) \alpha_{zz}(t) \rangle F_s(q, t) \quad (3)$$

$$I_{VH}^\alpha = \langle N \rangle \langle \alpha_{yz}^*(0) \alpha_{yz}(t) \rangle F_s(q, t) \quad (4)$$

In order to treat the scattering from molecules of arbitrary shape, it is convenient to use the spherical tensor formulation. Accordingly, the nine spherical components of the polarizability tensor, expressed in terms of the nine Cartesian components, are¹⁴

$$\begin{aligned} \alpha_0^{(0)} &= (1/3)^{1/2}(\alpha_{xx} + \alpha_{yy} + \alpha_{zz}) \\ \alpha_0^{(1)} &= 1/2(\alpha_{xy} - \alpha_{yx}) \\ \alpha_{\pm 1}^{(1)} &= \pm(1/8)^{1/2}((\alpha_{yz} - \alpha_{zy}) \pm i(\alpha_{zx} - \alpha_{xz})) \\ \alpha_0^{(2)} &= (1/6)^{1/2}(3\alpha_{zz} - (\alpha_{xx} + \alpha_{yy} + \alpha_{zz})) \\ \alpha_{\pm 1}^{(2)} &= \pm 1/2((\alpha_{xx} + \alpha_{zz}) \pm i(\alpha_{zy} + \alpha_{yz})) \\ \alpha_{\pm 2}^{(2)} &= 1/2((\alpha_{xx} - \alpha_{yy}) \pm i(\alpha_{xy} + \alpha_{yx})) \end{aligned} \quad (5)$$

The spherical components of the polarizability tensor in the laboratory frame (L) and molecule-fixed frame (B) can be related by the expression

$$\alpha_M^{(J)}(L, t) = \sum_{M'} (\alpha_{M'}^{(J)}(B, t)) (D_{M'M}^{(J)}(\Omega(t))) \quad (6)$$

where $D_{M'M}^{(J)}(\Omega(t))$ are functions of the Euler angles known as Wigner rotation functions. The $\alpha_{M'}^{(J)}(B, t)$ vary with time because of intramolecular motions that change the molecular polarizability anisotropy. The polarizability components in the laboratory frame ($\alpha_M^{(J)}(L, t)$) vary not only because of these changes in molecular polarizability

anisotropy but also because of overall molecular motion that changes the angular relationship between the laboratory frame and molecule-fixed frame (as given by the $D_{M'M}^{(J)}(\Omega(t))$).

Substitution of eq 5 and 6 into eq 3 and 4 shows that the spectrum depends on time correlation functions of the form

$$\langle [(\alpha_M^{(J)}(B, 0)) (D_{MK}^{(J)}(\Omega(0)))]^* \times [(\alpha_{M'}^{(J)}(B, t)) (D_{M'K'}^{(J)}(\Omega(t)))] \rangle \quad (7)$$

If we assume the overall rotation of the molecule is uncorrelated with the internal motions that cause fluctuations in the molecule's total polarizability, then (7) can be simplified to

$$\langle (\alpha_M^{(J)}(B, 0)) (\alpha_{M'}^{(J)}(B, t)) \rangle \times \langle (D_{MK}^{(J)}(\Omega(0))) (D_{M'K'}^{(J)}(\Omega(t))) \rangle \quad (8)$$

For convenience, the molecule-fixed axes may be chosen to diagonalize the overall rotational diffusion tensor $\tilde{\Theta}$; i.e.

$$\tilde{\Theta} = \begin{pmatrix} \Theta_{xx} & 0 & 0 \\ 0 & \Theta_{yy} & 0 \\ 0 & 0 & \Theta_{zz} \end{pmatrix}$$

Furthermore, assuming the dynamics roughly correspond to that of a symmetric diffusor (i.e., a rod), $\Theta_{xx} = \Theta_{yy} \equiv \Theta_{\perp}$ and $\Theta_{zz} = \Theta_{\parallel}$. Using the Debye model for rotational diffusion, we write the time correlation functions of the Wigner rotation functions for the symmetric diffusor as¹⁴

$$\begin{aligned} \langle (D_{MK}^{(J)}(\Omega(0))) (D_{M'K'}^{(J)}(\Omega(t))) \rangle &= \\ (2J + 1)^{-1} \delta_{MM'} \delta_{JJ'} \delta_{KK'} \times \\ \exp(-(J(J + 1)\Theta_{\perp} + M^2(\Theta_{\parallel} - \Theta_{\perp}))t) \end{aligned} \quad (9)$$

Using eq 5–9, we find that eq 3 and 4 become

$$I_{VV}^\alpha(q, t) = \langle N \rangle \alpha^2 F_s(q, t) + (4/3) I_{VH}^\alpha(q, t) \quad (10)$$

$$I_{VH}^\alpha(q, t) = (\langle N \rangle / 10) \sum_M \langle (\alpha_M^{(2)}(B, 0)) (\alpha_M^{(2)}(B, t)) \rangle \times (\exp(-6\Theta_{\perp} + M^2(\Theta_{\parallel} - \Theta_{\perp}))t) F_s(q, t) \quad (11)$$

where $\alpha = (1/3)(\alpha_{xx} + \alpha_{yy} + \alpha_{zz})$.

For $\theta^0 = 0$ (i.e., the unbroken rod), there is no flexing at the joint and consequently the polarizability of the molecule does not change with time. Thus $\alpha_M^{(2)}(B, 0) = \alpha_M^{(2)}(B, t)$ and $\langle (\alpha_M^{(2)}(B, 0)) (\alpha_M^{(2)}(B, t)) \rangle = |\alpha_M^{(2)}(B)|^2$. Furthermore, if we assume the rotational diffusion tensor and polarizability tensors are diagonal in the same molecule-fixed frame (a reasonable assumption for long, thin rods), $\alpha_{zz} = \alpha_{\parallel}$, $\alpha_{xx} = \alpha_{yy} = \alpha_{\perp}$, and the cross terms (α_{kl} , $k \neq l$) are zero. From eq 5, the only nonzero spherical components would be those for which $M = 0$. Thus, one obtains the usual result for a rigid, unbroken rod:

$$I_{VH}^\alpha(q, t) = (\langle N \rangle / 15) \beta^2 \exp(-6\Theta_{\perp} t) F_s(q, t) \quad (12)$$

where $\beta = \alpha_{\parallel} - \alpha_{\perp}$.

When the rod is allowed to bend, the polarizability tensor is no longer diagonal as the cross terms begin to contribute. The coordinate system for the combined polarizability of the two segments is chosen such that the polarizability tensor is diagonal at $\theta = 0$ and the percent contribution from each segment remains about the same as the rod bends. The axes pass through the joint, with the x and y axes in the plane that bisects the angle between the segments (see Figure 3). Each segment is cylindrically symmetric and has a segment-fixed diagonal polarizability tensor, $\tilde{\alpha}'$ and $\tilde{\alpha}''$. The segment-fixed tensors are transformed to the combined coordinate system (Figure 3) and added to form the total polarizability tensor, $\tilde{\alpha}$. In terms

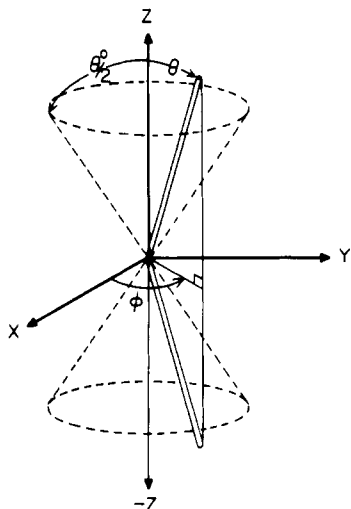


Figure 3. Coordinate system used for describing the bending motion. Each segment makes an angle θ with the z axis and the x and y axes are in the plane that bisects the angle between the segments.

of spherical coordinates, the Cartesian components of $\bar{\alpha}$ are

$$\begin{aligned}\alpha_{kl} &= n_k \bar{\alpha}' \cdot n_l + n_k \bar{\alpha}'' \cdot n_l \\ \alpha_{xx} &= (\alpha_{\parallel}' + \alpha_{\parallel}'') \sin^2 \theta \cos^2 \phi - (\alpha_{\perp}' + \alpha_{\perp}'') \sin^2 \theta \cos^2 \phi + (\alpha_{\perp}' + \alpha_{\perp}'') \\ \alpha_{yy} &= (\alpha_{\parallel}' + \alpha_{\parallel}'') \sin^2 \theta \sin^2 \phi - (\alpha_{\perp}' + \alpha_{\perp}'') \sin^2 \theta \sin^2 \phi + (\alpha_{\perp}' + \alpha_{\perp}'') \\ \alpha_{zz} &= (\alpha_{\parallel}' + \alpha_{\parallel}'') \cos^2 \theta + (\alpha_{\perp}' + \alpha_{\perp}'') \sin^2 \theta \\ \alpha_{xy} &= \alpha_{yx} = ((\alpha_{\parallel}' - \alpha_{\perp}') + (\alpha_{\parallel}'' - \alpha_{\perp}'')) \sin^2 \theta \sin \phi \cos \phi \\ \alpha_{xz} &= \alpha_{zx} = ((\alpha_{\parallel}' - \alpha_{\perp}') - (\alpha_{\parallel}'' - \alpha_{\perp}'')) \sin \theta \cos \theta \cos \phi \\ \alpha_{yz} &= \alpha_{zy} = ((\alpha_{\parallel}' - \alpha_{\perp}') - (\alpha_{\parallel}'' - \alpha_{\perp}'')) \sin \theta \cos \theta \sin \phi\end{aligned}\quad (13)$$

The α_{\parallel}' and α_{\perp}' are, respectively, the polarizabilities parallel and perpendicular to one segment's main axis and α_{\parallel}'' and α_{\perp}'' are the corresponding ones for the other segment. Thus, the spherical components of the total polarizability tensor can be found by substituting eq 13 into eq 5. The results for the $J = 0, 2$ components are

$$\begin{aligned}\alpha_0^{(0)} &= (1/3)^{1/2}((\alpha_{\parallel}' + \alpha_{\parallel}'') + 2(\alpha_{\perp}' + \alpha_{\perp}'')) = 3^{1/2}\alpha \\ \alpha_0^{(2)} &= (1/6)^{1/2}(((\alpha_{\parallel}' + \alpha_{\parallel}'') - (\alpha_{\perp}' + \alpha_{\perp}''))(3 \cos^2 \theta - 1)) \\ \alpha_{\pm 1}^{(2)} &= \mp(((\alpha_{\parallel}' - \alpha_{\perp}') - (\alpha_{\parallel}'' - \alpha_{\perp}'')) \sin \theta \cos \theta (\exp(\pm i\phi))) \\ \alpha_{\pm 2}^{(2)} &= \frac{1}{2}(((\alpha_{\parallel}' + \alpha_{\parallel}'') - (\alpha_{\perp}' + \alpha_{\perp}'')) \sin^2 \theta (\exp(\pm i2\phi)))\end{aligned}\quad (14)$$

A more convenient way of expressing eq 14 is in terms of the spherical $Y_{lm}(\Omega'(t))$, where $\Omega'(t)$ refers to the angles θ and ϕ . After this substitution, we obtain

$$\begin{aligned}\alpha_0^{(2)} &= (8\pi/15)^{1/2}(\beta' + \beta'') Y_{20}(\Omega'(t)) \\ \alpha_{\pm 1}^{(2)} &= (8\pi/15)^{1/2}(\beta' - \beta'') Y_{2\pm 1}(\Omega'(t)) \\ \alpha_{\pm 2}^{(2)} &= (8\pi/15)^{1/2}(\beta' + \beta'') Y_{2\pm 2}(\Omega'(t))\end{aligned}\quad (15)$$

where $\beta' = \alpha_{\parallel}' - \alpha_{\perp}'$, $\beta'' = \alpha_{\parallel}'' - \alpha_{\perp}''$.

From eq 15, the correlation functions for $\alpha_M^{(2)}$ in eq 11 can be written in terms of the time correlation functions of spherical harmonics:

$$\begin{aligned}\langle (\alpha_0^{(2)}(B,0))^* (\alpha_0^{(2)}(B,t)) \rangle &= (8\pi/15)^{1/2}(\beta' + \beta'')^2 \langle Y_{20}^*(\Omega'(0)) Y_{20}(\Omega'(t)) \rangle \\ \langle (\alpha_{\pm 1}^{(2)}(B,0))^* (\alpha_{\pm 1}^{(2)}(B,t)) \rangle &= (8\pi/15)^{1/2}(\beta' - \beta'')^2 \langle Y_{2\pm 1}^*(\Omega'(0)) Y_{2\pm 1}(\Omega'(t)) \rangle \\ \langle (\alpha_{\pm 2}^{(2)}(B,0))^* (\alpha_{\pm 2}^{(2)}(B,t)) \rangle &= (8\pi/15)^{1/2}(\beta' + \beta'')^2 \langle Y_{2\pm 2}^*(\Omega'(0)) Y_{2\pm 2}(\Omega'(t)) \rangle\end{aligned}\quad (16)$$

Thus, the bending motion is described by the autocorrelation functions of the $l = 2$ spherical harmonic functions of the bending angles. For the case where the break is a universal joint, other authors have shown that the correlation functions in eq 16 are about the same as those obtained when the break is complete (i.e., a solution of unconnected segments); only the time constants are significantly affected.¹⁻⁸ In other words, the segments move independently of one another, with respective rotational diffusion coefficients of D_r' and D_r'' . Thus, the correlation function for the case of the universal joint would be a sum of two exponentials with time decay constants of $6D_r'$ and $6D_r''$, one for each segment. When the decay constants are the same order of magnitude (i.e., when the two segments are about the same size), these two exponentials can be approximated by a single exponential with a decay constant of $3(D_r' + D_r'') = 6D_r$, i.e., the average of the two decay constants.

When there is a maximum bending angle of θ^0 , the problem can still be treated in terms of a single segment with a rotational diffusion coefficient of D_r if it is assumed the segments still move independently of one another. However, now the segment diffuses within a conical volume, with a maximum angle from the axis of the cone of $\theta^0/2$. Assuming free rotational diffusion within the cone, Wang and Pecora¹⁵ have calculated the time correlation functions of the spherical harmonics for this system. The correlation functions for $l = 2$ are

$$\begin{aligned}\langle Y_{20}^*(\Omega'(0)) Y_{20}(\Omega'(t)) \rangle &= (5/4\pi) \sum_{n=1}^{\infty} C_n^0 \exp(-\nu_n^0(\nu_n^0 + 1)D_r t) \\ \langle Y_{2\pm 1}^*(\Omega'(0)) Y_{2\pm 1}(\Omega'(t)) \rangle &= (5/8\pi) \sum_{n=1}^{\infty} C_n^1 \exp(-\nu_n^1(\nu_n^1 + 1)D_r t) \\ \langle Y_{2\pm 2}^*(\Omega'(0)) Y_{2\pm 2}(\Omega'(t)) \rangle &= (5/8\pi) \sum_{n=1}^{\infty} C_n^2 \exp(-\nu_n^2(\nu_n^2 + 1)D_r t)\end{aligned}\quad (17)$$

The C_n^m and ν_n^m depend on the angle $\theta^0/2$ (see ref 15). For $(\theta^0/2) \leq 80^\circ$, the following expressions are valid:

$$\begin{aligned}C_1^0 &= (1/4)\mu_0^2(1 + \mu_0)^2 \\ \mu_0 &= \cos(\theta^0/2)\end{aligned}$$

$$\begin{aligned}\sum_{n=2}^{\infty} C_n^0 &= (1/20)(4 - \mu_0 - 6\mu_0^2 - \mu_0^3 + 4\mu_0^4) = C_2^0 \\ \sum_{n=1}^{\infty} C_n^1 &= (1/5)(2 + 2\mu_0(1 + \mu_0) - 3\mu_0^3(1 + \mu_0)) \approx C_1^1 \\ \sum_{n=1}^{\infty} C_n^2 &= (1/20)(8 - 7\mu_0(1 + \mu_0) + 3\mu_0^3(1 + \mu_0)) = C_1^2\end{aligned}\quad (18)$$

Thus, for this limit on θ^0 , only the C_1^0 , C_2^0 , C_1^1 , and C_1^2

terms are important. Furthermore, $\nu_1^0 = 0$ for all values of θ^0 ; thus, the C_1^0 term is time independent. Substituting eq 17 into eq 16, one obtains the autocorrelation functions for the $\alpha_m^{(2)}$:

$$\begin{aligned} \langle (\alpha_0^{(2)}(0)) * (\alpha_0^{(2)}(t)) \rangle &= (2/3)(\beta' + \beta'')^2(C_1^0 + C_2^0 \exp(-\nu_2^0(\nu_2^0 + 1)D_t t)) \\ \langle (\alpha_{\pm 1}^{(2)}(0)) * (\alpha_{\pm 1}^{(2)}(t)) \rangle &= (1/3)(\beta' - \beta'')^2(C_1^1 \exp(-\nu_1^1(\nu_1^1 + 1)D_t t)) \\ \langle (\alpha_{\pm 2}^{(2)}(0)) * (\alpha_{\pm 2}^{(2)}(t)) \rangle &= (1/3)(\beta' + \beta'')^2(C_1^2 \exp(-\nu_1^2(\nu_1^2 + 1)D_t t)) \quad (19) \end{aligned}$$

When these correlation functions are inserted into eq 11, we obtain

$$\begin{aligned} I_{VH}^a(q, t) &= (\langle N \rangle / 15) ((\beta' + \beta'')^2(C_1^0 + C_2^0 \exp(-\nu_2^0(\nu_2^0 + 1)D_t t) \exp(-6\theta_{\perp} t) + \\ &(\beta' - \beta'')^2 C_1^1 \exp(-\nu_1^1(\nu_1^1 + 1)D_t t) \exp(-(5\theta_{\perp} + \theta_{\parallel})t) + \\ &(\beta' + \beta'')^2 C_1^2 \exp(-\nu_1^2(\nu_1^2 + 1)D_t t) \times \\ &\exp(-(2\theta_{\perp} + 4\theta_{\parallel})t)) F_s(q, t) \quad (20) \end{aligned}$$

From eq 18, as $\theta^0 \rightarrow 0$, $C_1^0 \rightarrow 1$ and all the other C_n^m 's go to zero, once again giving the result for the unbroken rod (eq 12, $\beta = \beta' + \beta''$).

If the two segments have roughly the same anisotropy ($\beta' \approx \beta''$), the $m = \pm 1$ term will be small compared to the others and can be neglected. Furthermore, since $\nu_1^2 \approx \nu_2^0$ and $\theta_{\parallel} \gg \theta_{\perp}$ for long rods,^{16,17} the $m = \pm 2$ term appears on a much faster time scale than the $m = 0$ term and thus should be readily time resolvable; i.e., a time scale suitable for measuring the $m = 0$ component should have little contribution left from the $m = \pm 2$ component. Dropping these $m \neq 0$ terms and substituting $F_s(q, t) = \exp(-q^2 D_t t)$, we obtain from eq 20 and 10

$$I_{VV}^a(q, t) = \langle N \rangle \alpha^2 e^{-q^2 D_t t} + (4/3) I_{VH}(q, t) \quad (21)$$

$$\begin{aligned} I_{VH}(q, t) &= (\langle N \rangle / 15) \times \\ &(\beta' + \beta'')^2 (C_1^0 + C_2^0 \exp(-\nu_2^0(\nu_2^0 + 1)D_t t)) e^{-q^2 D_t t - 6\theta_{\perp} t} \quad (22) \end{aligned}$$

The homodyne scattered light intensity time correlation functions would be proportional to the square of eq 21 and 22;¹⁴ i.e.

$$I_{VV}(q, t) = A(I_{VV}^a(q, t))^2 + B \quad (23)$$

$$I_{VH}(q, t) = A'(I_{VH}^a(q, t))^2 + B' \quad (24)$$

where A , B , A' , and B' are constants for a given q and incident light intensity.

Results

The details of the experiment are given elsewhere.¹³ The polarized and depolarized homodyne autocorrelation functions were fit by nonlinear least-squares analysis to the equations

$$C(t) = A + B \exp(-2t/\tau) \quad (25)$$

$$C(t) = A + B_1 \exp(-2t/\tau_1) + B_2 \exp(-2t/\tau_2) \quad (26)$$

$$C(t) = A + (B_1' \exp(-t/\tau_1') + B_2' \exp(-t/\tau_2'))^2 \quad (27)$$

where A , B , B_1 , B_1' , B_2 , and B_2' are constants for a given q , incident light intensity, and concentration, τ_1 , τ_2 , τ , τ_1' , and τ_2' are time constants, and t is the time. The results for myosin rod are tabulated in Tables I and II, along with the values obtained for the free segments (i.e., LMM and S-2).

Assuming eq 12 is applicable, a single-exponential fit to the depolarized data (eq 25) yields values for θ_{\perp} (Table

Table I
Rotational Diffusion Coefficients for Myosin Rod and Its Fragments, Assuming One Decay Time

fragment	contour length, ^a nm	$\Theta_{\perp 20, w}$, krad/s	
		theory ^b	expt ^{c, d}
LMM	78.5	23.2	21.7 ± 0.8, ^c 21.8 ± 0.3 ^d
S-2	65.0	38.2	47.5 ± 1.6 ^d
rod	136.0	5.3	7.7 ± 0.8, ^c 6.9 ± 0.1 ^d

^a The contour length is based on electron micrograph data.²¹ ^b Θ_{theory} is based on Broersma's relations for a dilute solution of rods, using the contour length and a diameter of 2 nm.¹⁸⁻²⁰ ^c From our light scattering measurements.¹³ ^d From electric birefringence data,¹⁰ correcting the results for viscosity and temperature (3–20 °C).

Table II
Depolarized Decay Constants for Myosin Rod, Assuming Two Decay Times

type of fit	$1/\tau_1$, ks ⁻¹	$1/\tau_1'$, ks ⁻¹	$1/\tau_2'$, ks ⁻¹	B_1/B_2	B_1'/B_2'
eq 25 ^a			34 ± 5		
eq 26	178 ± 36	329 ± 72	27 ± 5	3.2 ± 1.0	1.6 ± 0.5
eq 27		319 ± 84	28 ± 6		1.2 ± 0.4

^a The fits were done for time $t > 8 \mu\text{s}$.

I). Clearly, the value for myosin rod is faster than one would predict for a stiff, unbroken rod. The myosin rod's value for $q^2 D$ was found from polarized light scattering measurements¹³ (assuming a single exponential) to be $4.8 \pm 0.8 \text{ ks}^{-1}$, somewhat lower than the infinite-dilution value predicted by Broersma's relations for an unbroken rod¹⁸⁻²⁰ (the predicted value for the conditions of these experiments is 8.0 ks^{-1}). The correlation functions for the depolarized scattered light from the myosin rod were better described by two time constants. Naturally, the root-mean-square error was less for the two-exponential fits; one almost always improves the fit by using more variables, especially for noisy data. In this case, however, the single-exponential fit gave different time constants for different time scales of the measurement, while the two-exponential fits were independent of the time scale of the measurement. Table II gives the values obtained for the decay times when the depolarized correlation functions are fit to eq 26 and 27. If we assume the first exponential in eq 26 is the cross term of the two exponentials squared in eq 27 (i.e., $2/\tau_1 = 1/\tau_1' + 1/\tau_2'$, $\tau_2 = \tau_2'$, $B_2 = (B_2')^2$ and $B_1 = 2B_1'B_2'$), both fits yield the same values for the decay time and the preexponential factors, within experimental error (see Table II). The first exponential found from eq 26 does have somewhat more amplitude and a slightly faster time constant than the cross term from eq 27 would have, due to a slight contribution from the fastest term in eq 27 [$\exp(-(2t/\tau_1'))$]. Since eq 27 is the theoretical form expected for the homodyne correlation functions, its parameters were used for all subsequent analysis. Finally, a single-exponential fit was done on the data in which only points with $t > 8 \mu\text{s}$ were used, thus eliminating most of the contribution from the first exponential and yielding a more reliable value for the slower time.

The ratio B_1'/B_2' (where τ_1' is the faster time) in eq 27 should correspond to the ratio C_2^0/C_1^0 in eq 22. From experiment, $B_1'/B_2' = 1.2 \pm 0.4$. This corresponds to an average angle θ^0 of 128° (ranging from 121 – 132°). From Pal's equations,^{22,23} the value of ν_2^0 at 128° was found to be $2.97 \approx 3$. Using this value for ν_2^0 and the values found

for the decay constants, we obtain a value for D_r of 24 ± 6 krad/s. The rotational diffusion constants for LMM and S-2 free in solution have been measured (Table I);^{10,13} the average of their values is about 35 krad/s. Thus, the value obtained for D_r is about 69% of this average value. For the case where the break is a universal joint between two identical segments, the theoretical effect of the joint on the rotational diffusion coefficients of the segments has been calculated.^{1,7,8} There are two major distinctions between a dilute solution of once-broken rods and one of unconnected segments. First of all, the relationships between center-of-mass (translational) motions and the orientational motions of the segments are different. Second, there exists some hydrodynamic interaction between connected segments that is not present for the free segments. As a result, the rotational diffusion coefficient for a connected segment is expected to be smaller than the value for an unconnected segment. Wegener et al.⁸ predict that D_r for a connected segment would be 78% of the value for an unconnected segment, while Fujiwara et al.,⁷ from a more detailed accounting of the hydrodynamic interactions, predict that D_r is 53% of that for an unconnected segment. Thus, the value obtained for D_r is consistent with the current theories.

The slow time in the two-exponential fit roughly corresponds to the overall rotational diffusion of the myosin rod. As a result of the difficulties involved in fitting two exponentials to noisy data, the value for Θ_{\perp} obtained from the second exponential (3.7 ± 0.8 krad/s) may be somewhat low. The value obtained by fitting a single exponential to the long-time tail of the correlation function ($t > 8 \mu\text{s}$) is 4.8 ± 0.8 krad/s. Considering the theoretical approximations, both values agree well with the value predicted if myosin were a stiff, unbroken rod (5.3 krad/s).

Conclusions

A simple, approximate theory has been formulated for the dynamic light scattering correlation functions of a once-broken rod whose angle of bend is restricted. We obtain good agreement between this theory and the dynamic light scattering results for myosin rod. The limit of large θ^0 also appears to be consistent with the results for once-broken rods with no restriction on the intersegmental angle.⁷ Further experiments on other once-broken rod systems could be performed to check the validity of this theory. Theoretically, the effect of adding a harmonic restoring force to the joint can be determined. In addition, more explicit consideration of the hydrodynamic interactions and the effect of coupling between the various motions can be incorporated into the theory.

Acknowledgment. We thank Dr. C.-C. Wang and Professor Stefan Highsmith for providing the experimental data. We also thank Professor H. L. Frisch and Dr. Susan G. Stanton for their critique of this work. This work was supported by National Science Foundation Grant No. NSF CHE 79-01070 and National Institutes of Health Grant No. NIH 5R01 GM 22517.

Appendix. Effects of Coupling between Translation, Rotation, and Bending

Coupling between rotation and translation might arise because of the anisotropy of translational diffusion. For instance, a rod-shaped molecule might have a different translational diffusion coefficient for motion parallel to its long axis (D_{\parallel}) from that for motion perpendicular to it (D_{\perp}). Several studies of rotation–translation coupling due

to this translational anisotropy have been performed for rigid rods.^{14,25–27} The rigid-rod case may serve to give a rough estimate of the coupling for the flexing rod.

Let $\gamma = q^2(\Delta D/\Theta)$, where Θ is the rod rotational diffusion coefficient, q is the scattering vector length, and $\Delta D \equiv D_{\parallel} - D_{\perp}$. In the absence of intramolecular interference, the contribution of terms dependent on this coupling to the polarized and depolarized correlation functions would go roughly as $\gamma^2/100$ and $\gamma^2/1000$, respectively.^{26,27} Thus, for $\gamma < 1$, the contribution of these higher order terms is less than 1% of the total scattering. If the myosin rod were stiff and unbroken, assuming that $D_{\perp} \approx 1/2 D_{\parallel}$, we find that for the condition of our experiment

$$\gamma \approx 3/4 q^2 D/\Theta \approx 1.2$$

For a once broken-rod, the translational diffusion is similar to that for an unbroken rod of equivalent chain length.²⁴ However, in addition, the translational anisotropy ΔD should actually decrease as the average shape of the particle becomes more spherical. We thus expect that ignoring the translational–rotational coupling will lead to errors of only about 1% in the polarized correlation functions and of about 0.1% in the depolarized results.

Since as noted above, the translational diffusion coefficient of a once-broken rod is not very different (at most 10% larger) from that of a stiff rod,²⁴ we do not think it likely that coupling between bending and translation will have a major effect on the light scattering time correlation functions.

By analogy, we expect the terms coupling bending to rotation to contribute to the correlation functions roughly as $(\Theta/D_R)^2$, where D_R is the bending diffusion coefficient. For myosin rod this is of the order of 4%.

References and Notes

- (1) Yu, H.; Stockmayer, W. H. *J. Chem. Phys.* **1967**, *47*, 1369.
- (2) Teremoto, A.; Yamashita, T.; Fujita, H. *J. Chem. Phys.* **1967**, *46*, 1919.
- (3) Pecora, R. *Macromolecules* **1969**, *2*, 31.
- (4) Hassager, O. *J. Chem. Phys.* **1969**, *60*, 2111.
- (5) Matsumoto, T.; Nishioka, N.; Teremoto, A.; Fujita, H. *Macromolecules* **1974**, *7*, 824.
- (6) Fujiwara, M.; Saito, N. *Polym. J.* **1979**, *11*, 249.
- (7) Fujiwara, M.; Numasawa, N.; Saito, N. *Rep. Prog. Polym. Phys. Jpn.* **1980**, *23*, 531.
- (8) Wegener, W.; Dowben, R.; Koester, V. *J. Chem. Phys.* **1980**, *73*, 4086.
- (9) Gergely, J. *Fed. Proc., Fed. Am. Soc. Exp. Biol.* **1950**, *9*, 176.
- (10) Highsmith, S.; Kretzschmar, K. M.; O'Konski, C. T.; Morales, M. F. *Proc. Natl. Acad. Sci. U.S.A.* **1977**, *74*, 4986.
- (11) Elliott, A.; Offer, G. *J. Mol. Biol.* **1978**, *123*, 505.
- (12) Takahashi, K. *J. Biochem.* **1978**, *83*, 905.
- (13) Highsmith, S.; Wang, C.-C.; Zero, K.; Pecora, R.; Jardetzky, O. *Biochemistry* **1982**, *21*, 1192.
- (14) Berne, B. J.; Pecora, R. "Dynamic Light Scattering"; Wiley: New York, 1976.
- (15) Wang, C.-C.; Pecora, R. *J. Chem. Phys.* **1980**, *72*, 5333.
- (16) Perrin, F. *J. Phys. Radium* **1934**, *5*, 497.
- (17) Price, C.; Heatly, F.; Holton, T. J.; Harris, P. A. *Chem. Phys. Lett.* **1977**, *49*, 504.
- (18) Broersma, S. *J. Chem. Phys.* **1960**, *32*, 1626.
- (19) Broersma, S. *J. Chem. Phys.* **1960**, *32*, 1632.
- (20) Newman, J.; Swinney, H. L.; Day, L. A. *J. Mol. Biol.* **1977**, *116*, 593.
- (21) Lowey, S.; Slayter, H. S.; Weeds, A. G.; Baker, H. *J. Mol. Biol.* **1969**, *42*, 1.
- (22) Pal, B. *Bull. Calcutta Math. Soc.* **1919**, *9*, 2.
- (23) Pal, B. *Bull. Calcutta Math. Soc.* **1919**, *10*, 3.
- (24) Yamakawa, H. "Modern Theory of Polymer Solutions"; Harper and Row: New York, 1971; p 328.
- (25) Loh, E. *Biopolymers* **1979**, *18*, 2569.
- (26) Lee, W.; Schmitz, K.; Lin, S.-C.; Schurr, J. M. *Biopolymers* **1977**, *16*, 583.
- (27) Zero, K.; Pecora, R. *Macromolecules* **1982**, *15*, 87.